Theory and computation of electron correlation in the continuous spectrum: Double photoionization cross section of H⁻ and He near and far from threshold

Cleanthes A. Nicolaides,[*] Costas Haritos, and Theodoros Mercouris

Theoretical and Physical Chemistry Institute, National Hellenic Research Foundation, 48, Vasileos Constantinou Avenue, 116 35 Athens, Greece

We present a theoretical approach to the *ab initio* calculation of single or multiphoton double electron ionization cross sections, $\sigma^{++}(E)$, of polyelectronic atoms, near (Wannier region) and far from threshold. The overall computational method is variational, uses functions of real as well as of complex coordinates, and follows the many-electron, many-photon theory proposed by Mercouris and Nicolaides [J. Phys. B **21**, L285 (1988); **23**, 2037 (1990)]. It incorporates the electronic structure and the pair correlations in the continuum via configuration-interaction techniques. $\sigma^{++}(E)$ is obtained as the imaginary part of a complex eigenvalue that is computed by diagonalizing a state-specific non-Hermitian matrix constructed from separately optimized function spaces Q and P representing the field-induced resonance state. Q contains correlated wave functions of bound or quasibound states expanded over numerical and analytic orbitals of real coordinates. P is composed, in principle, of subspaces P_1 and P_2, representing the one- and the two-electron channels, respectively, which are optimized separately and then are allowed to mix via the construction of the total non-Hermitian matrix. Both are spanned by basis sets of real coordinates for the ionized core and of complex coordinates for the outgoing part of the one- and the two-electron resonance state. The two-electron square integrable ''continuum'' function space is made orthogonal to the available single electron channels in order for $\sigma^{++}(E)$ not to include portions of the single electron ionization cross section $\sigma^{+}(E)$. Application is made to the single photon $\sigma^{++}(E)$ of the prototypical systems H⁻ and He, but without the mixing of P_2 and P_1, due to numerical instabilities. The two-electron ionization channels were composed of Slater-type orbitals, symmetry-coupled according to (sp), (pd), and (df). Higher symmetries would also be needed at higher energies, with corresponding increase of angular correlation terms in the initial-state wave function. The continuous energy ranged from $E=0$ to $E=250$ eV. In the threshold region $E=0–2$ eV, the length and velocity results are in good agreement with experiment for H⁻ and in reasonable agreement with experiment for He. Far from threshold, there is discrepancy between length and velocity forms in this as well as in previous works by other methods. Apart from whatever inadequacies of the basis functions, this is possibly due to the exclusion of mixing of the single electron open channels into the correlated wave function of the two free electrons. By comparing the results from the use of correlated wave functions with those obtained when the calculation of the transition matrix element is done with wave functions of real coordinates, where the initial state is correlated but the final one is only a product of Coulomb wave functions, the effect of correlation of the two free electrons is deduced for the case of He, without considering the mixing of one- and two-electron channels. Finally, a by-product of the present development was the calculation of the He $\sigma^{+}(E)$ to the $n=1$ single ionization threshold. Comparison with previous accurate experimental results reveals very good agreement. [S1050-2947(97)05904-0]

PACS number(s): 32.80.Fb, 32.90.+a

I. INTRODUCTION

When atoms or molecules with N electrons ($N \geq 2$) are probed by energetic photons or electrons and other particles or by intense laser light (multiphoton absorption), there is finite probability of producing final states with two or more free electrons. Such processes give rise to significant and challenging theoretical problems as regards the *ab initio* calculation of the related transition rates, especially for the near threshold region.

In this paper, we present a theory and method of calculation of the *cross section of double photoionization*, $\sigma^{++}(E)$, of ground or excited N-electron states by one or more photons. The application demonstrating the approach is to the one-photon ionization of the H⁻ and He ¹S ground states that constitute the prototypical cases (especially He) for the application of a number of theoretical approaches and for experimental measurement. The continuous energy spectrum that was studied ranges from threshold ($E=0$) (relevant to the so-called *Wannier problem*—see Sec. IV) to 250 eV. Although this application of the method has as object the ¹S ground state of two-electron atoms, the structure of the theory is such that it allows the computation of $\sigma^{++}(E)$ for arbitrary atomic states. This is because both the zeroth-order functions as well as electron correlation in the discrete and the continuous spectrum are represented by expansions over symmetry-adapted configurations with optimized numerical or analytic orbitals. For example, such a theory is capable of dealing reliably with the excited states as well. If excited states are metastable, they can be used as initial states. Or,

---

*Also at Physics Department, National Technical University, Athens, Greece.

they can act as intermediate states during multiphoton processes and serve as the last step before multielectron ejection.[1]

When examining the problem of computing the one-photon $\sigma^{++}(E)$, two major factors that must be dealt with and understood quantitatively emerge. First, is the issue of being able to compute systematically to all orders (at least in principle) and not just within an approximate model, the energy-dependent interaction of the two free electrons in the field of the remaining ionic state. To be complete, such a calculation must also incorporate the effect of mixing of single electron continua or of autoionizing states belonging to other thresholds into the wave function of the final state with two free electrons. Second is the issue of being able to recognize and compute the important for the process, electronic structure and electron correlation effects.

A number of theoretical approaches to the calculation of $\sigma^{++}(E)$ have been published, especially for the He $1s^2$ ^1S state where both the initial and the final state can be subjected to special methods (e.g., use of r_{12}-dependent terms) [2–16]. For atomic states with many electrons, thus far only the works based on the methods of diagrammatic many-body perturbation theory have provided results where a portion of the interactions was accounted for ([5] and references therein). (See also Ref. [17] for an approximate wave function calculation of $\sigma^{++}(E)$ to only one channel for the open shell He$^-$ $1s2s2p$ $^4P^o$, showing that two-electron ionization transitions are described semi-quantitatively even when just Hartree-Fock (HF) functions are employed, i.e., without the inclusion of electron correlation.)

A general observation that can be made based on the results of [2–17] is that, even for the He ^1S case, the sensitivity of the calculation of $\sigma^{++}(E)$ is such that the length and velocity forms of the dipole transition operator produce rather different results. For example, Kornberg and Miraglia [13], who employed r_{12}-dependent wave functions for initial and final states, state in their paper that ''*For all energies, the results exhibit a large discrepancy between the length and velocity forms.*'' The literature [2–24] also reveals the existence of an important open problem, i.e., that of developing and applying a quantum-mechanical method for the accurate calculation of $\sigma^{++}(E)$ in the near threshold region (say $E=0$–2 eV), whereby electronic structure as well as electron correlation in initial and final states are accounted for (see Sec. IV).

II. PRESENT THEORY

A. State-specific electronic structure, nonorthonormality, and electron correlation

The overall method implementing the present theory is variational, and is based on the use of appropriately chosen square-integrable function spaces composed of one-electron functions of real and complex coordinates. Before we show how this is done, we consider the first step, that of understanding *a priori* the most important configurations that must be included in the calculation of $\sigma^{++}(E)$. Once these have been chosen, it is expected that the bulk of the contributions to $\sigma^{++}(E)$ can be accounted for. The remaining parts can then be added systematically by augmenting the relevant expansions according to the desired computational effort.

The guidelines for carrying out this sort of analysis follow from the first-order theory of oscillator strengths (FOTOS) [25,26], which allows the recognition and calculation to all orders (variationally) of the major features of the interplay between electronic structure and photoexcitation dynamics.

In the following heuristic arguments, we assume that the bound and the two-electron scattering wave functions are available. Consider the amplitude of one-photon, two-electron photoionization, $\langle \Psi_i | \vec{D} | \Psi_f(E) \rangle$, where $\vec{D}$ is the dipole operator. Ψ_i is the exact wave function for the initial bound state. $\Psi_f(E)$ is the exact wave function for the final scattering state of energy E. For an N-electron state it can be written as

$$\Psi_f(E) = \mathcal{A}[\Phi_{\text{core}}(N-2) \otimes \Psi(r_1, r_2; E)], \qquad (1)$$

where $\Phi_{\text{core}}(N-2)$ is the wave function of the ionized bound state and $\Psi(r_1, r_2; E)$ is the two-electron scattering function coupled to $\Phi_{\text{core}}(N-2)$. $\mathcal{A}$ is the N-electron antisymmetrizer. According to FOTOS, let us expand to first order both Ψ_i and $\Psi_f(E)$, where the zeroth-order functions Ψ_i^0 and $\Psi_f^0(E)$ are multiconfigurational and contain the major correlation effects:

$$\Psi_i \approx \Psi_i^0 + \sum_n n > \frac{\langle n | H | \Psi_i^0 \rangle}{\Delta E_n}, \qquad (2a)$$

$$\Psi_f(E) \approx \Psi_f^0(E) + \sum_m m > \frac{\langle m | H | \Psi_f^0(E) \rangle}{\Delta E_m}. \qquad (2b)$$

The configurations (channels) entering in Ψ_i^0 and $\Psi_f^0(E)$ constitute the state-specific N-electron Fermi seas. For example, in He, Ψ_i^0 consists of the $1s^2$, $2s^2$, $2p^2$ configurations with radials obtained self-consistently, while $\Psi_f^0(E)$ consists of the $\varepsilon s \varepsilon' p$ and $\varepsilon p \varepsilon' d$ open channels, at least at the low-energy part of the continuous spectrum. In general, the Fermi-sea configurations in the continuum may interfere and mix with autoionizing states and with single photoionization channels.

Substitution of expressions (2a) and (2b) into the transition amplitude then allows the *a priori* recognition to a good degree of reliability of the *form* of the important vectors $|n\rangle$ and $|m\rangle$, according to the following criteria.

(1) Nonorthonormality integrals, resulting from the state-specific nature of each wave function. For example, two-electron excitation and ionization can be semiquantitatively described without resort to electron correlation since even with just a Hartree-Fock wave function a rough estimate of the transition amplitude can be obtained [17,25–27]. Furthermore, consideration of the degree of nonorthonormality leads to recognition of the role played by pair correlations beyond the zeroth-order description. (If relatively accurate dipole matrix elements involving multiply excited states are required, state-specific small expansions for Ψ^0 seem to be sufficient [27].)

(2) Bound-bound and bound-free dipole and Hamiltonian matrix elements. For example, consider the $1s^2$ configuration, which is the dominant configuration in the Fermi sea of the ^1S ground state. The first-order transition amplitude consists of matrix elements of the type

$$\langle 1s^2|\vec{D}|m\rangle \frac{\langle m|H|\varepsilon\varepsilon'p\rangle}{\Delta E_m}. \tag{3}$$

The form (3) implies that, to a very good approximation, apart from the Fermi-sea configurations, the $|m\rangle$ functions have the form $1s\sigma_p$, where σ_p is a one-electron function of p symmetry. For example, due to its relatively large oscillator strength, a non-negligible contribution to Eq. (3) comes from the $1s2p$ configuration. Therefore, if high accuracy is desired, the structure of the theory must be such that it allows the inclusion of higher-order terms representing low-lying bound states. Of course, this would be relevant for He. For the negative ion, H$^-$, such bound states do not exist. (See Refs. [28, 29] for field-induced properties where the function spaces included such excitations for He but not for H$^-$.)

Correspondingly, using for the sake of example one of the two major final-state configurations, the $\varepsilon s\varepsilon'p$, we obtain

$$\langle \varepsilon s\varepsilon'p|\vec{D}|n\rangle \frac{\langle n|H|1s^2\rangle}{\Delta E_n}. \tag{4}$$

In this case, symmetry together with Brillouin's theorem for the unimportance of the single excitations $1ss'$ show that continuum configurations of ^1S symmetry, $(\varepsilon s\varepsilon's)$, do not contribute. However, in general, for other atomic states with open shells and heavy zeroth-order configurational mixing, dipole transition matrix elements involving the continuous spectrum due to higher-order effects should acquire importance.

Finally, we stress that the state-specific electronic structure methods (e.g., [26,30,31]) allow the economical calculation of reliable wave functions for a variety of ground or excited states in which the ionized atom may be found after the double photoionization. These functions should form the input for calculation not only of the dipole matrix elements but also of the Coulomb interaction ones, when consideration is given to interchannel coupling (e.g., upon double photoionization of Ne ^1S, the final $^1P^o$ states correspond to the coupling of the two free electrons to Ne^{2+} core terms such as $1s^22s^22p^4$ $^3P,^1D,^1S$, $1s^22s2p^5$ $^{3,1}P^o$, $1s^22s^22p^33l$ ^{2S+1}L, etc.).

B. The general framework: Construction and diagonalization of state-specific non-Hermitian matrices with complex eigenvalues

A fundamental question for the problem treated in this paper is how to calculate systematically the important for $\sigma^{++}(E)$ *localized correlation effects* in arbitrary atomic states, once these have been identified as playing a certain role in the photoionization process. The analysis given in the Sec. II A, in conjunction with the related information contained in [25,26,31], should guide the reader as regards the efficient calculation of the relevant bound wave functions of arbitrary structures. An important element of the state-specific theory ([31], and references therein) for the calculation of correlated wave functions is that the Fermi-sea orbitals, which enter in the overall calculation as zero-order orbitals and contribute the most to the property of interest, are obtained numerically [30].

The other, and heretofore outstanding, aspect of the problem of developing theory and methods for the *ab initio* calculation of $\sigma^{++}(E)$, is how to incorporate to *all orders* the multielectron interactions that include the two free electrons. Given our earlier proposals and experience on the computation to all orders of field-induced observable properties via the diagonalization of appropriately constructed state-specific non-Hermitian matrices (e.g., [1,28,29,32,33]), we considered that $\sigma^{++}(E)$ could also be computed by modifying and implementing such methods, where the aim is to obtain complex energies whose imaginary part is associated with *partial* or with *total* widths.

The essential formal picture is the following: The initially discrete state is dressed by an ac field with photon energy $(\hbar\omega)$ corresponding to the double-ionization threshold (for H$^-$, $I^{++}=14.36$ eV, for He, $I^{++}=79.00$ eV), plus a range of total-energy E. The field-dressed state becomes energetically degenerate with both the one-electron and the two-electron continua, with which it interacts via the electric-dipole interaction operator. Such a situation, i.e., that of a discrete level interacting with adjacent free particle continua, represents the physics of a variety of phenomena caused by nonstationary states whose energies, energy shifts, and energy widths (transition rates) can be obtained from the solution for the complex energies of appropriately defined state-specific non-Hermitian Hamiltonian matrices (e.g., [1,28,29,32]). The matrix elements of these matrices are evaluated over functions of real and of complex coordinates with $\varrho^*=re^{-i\theta}$. In fact, the $\varrho=re^{i\theta}$ transformation can be effected beyond a certain radius R, which is defined either arithmetically or via the choice of localized basis sets, a procedure proposed by Nicolaides and Beck [34] as a possible practical tool for the better understanding of resonance functions in multielectron systems and for the development of computational approaches [34]. The region defined by an effective R is spanned by N-electron functions of real coordinates. The conceptual framework of defining and calculating separately (at first) function spaces whose sum constitutes a state-specific resonance wave function whose outgoing wave is represented by a basis with complex coordinates, has been used for the development of the many-electron, many-photon theory (MEMPT) (e.g., [28,32]). The same spirit was followed in the recently proposed R-matrix Floquet theory of multiphoton processes [35].

Using this background and its numerous successful applications, we assume that in the case of two (or more) electron emissions, induced by one or more photons, there is a dressed state and a corresponding resonance wave function that can be made square integrable by performing the ϱ^* transformation on the coordinates of each of the two outgoing electrons. Furthermore, it is assumed, as in the case of bound-state problems of atomic and molecular physics, that this square integrable pair function can be expanded in terms of one-electron functions of the usual type, such as Slater or Laguerre orbitals. Of course, it should be expected that such a representation of the scattering part of a two-electron resonance function is not as easily achievable as that of a two-electron function corresponding to a ground state. However, these are only the initial theoretical steps and additional experience is expected to be accumulated by further calculations.

TABLE I. Single photoionization cross section of He (in Mb) as a function of photon energy (in eV). Column 2 contains the experimental values by Samson *et al.* [41]. Columns 3 and 4 contain the results of this work where the interaction Hamiltonian, in the dipole approximation, is from the length and velocity forms, respectively.

Photon energy (eV)	Cross section (Mb) experiment (Ref. [41])	Cross section (Mb) this work, length form	Cross section (Mb) this work, velocity form
24.587	7.40	7.27	7.20
25	7.21	7.00	6.90
26	6.79	6.71	6.56
27	6.40	6.32	6.17
28	6.05	5.97	5.82
29	5.70	5.65	5.51
30	5.38	5.34	5.20
31	5.10	5.06	4.92
32	4.82	4.79	4.66
33	4.57	4.54	4.40
34	4.32	4.31	4.17
35	4.09	4.09	3.96
36	3.88	3.88	3.75
37	3.68	3.69	3.56
38	3.50	3.51	3.39
39	3.32	3.34	3.23
40	3.16	3.18	3.07
45	2.48	2.52	2.42
50	2.02	2.03	1.94
55	1.67	1.66	1.58
59	1.56	1.42	1.35
65	1.20	1.14	1.08
70	0.975	0.967	0.908
80	0.693	0.705	0.658
90	0.516	0.528	0.534
100	0.393	0.405	0.379
120	0.244	0.252	0.232
150	0.131	0.137	0.125
200	0.055	0.060	0.055
250	0.027	0.031	0.028

According to the above, the form of the trial wave function Ψ, which is square integrable and is connected adiabatically to the initial-state wave function Ψ_0, is

$$\Psi(\vec{r},\vec{\rho}*)=\sum_{i,n} \alpha_{i,n}(\theta)\Phi_i(\vec{r});n\rangle+\sum_{j,n} b_{j,n}(\theta)X_j(\vec{r},\vec{\rho}*);n\rangle. \quad (5)$$

The Φ_i represent bound or quasibound states and are functions of real coordinates, collectively represented by $\vec{r}$. X_j represents open channels and have the form of Eq. (1) for two free-electron continua (let us denote them by X_j^{++}), and an analogous one, denoted by X_j^+, for one free-electron continua (e.g., for He, single-electron continua are $1s\varepsilon p$, $2s\varepsilon p$, $2p\varepsilon d$, $2p\varepsilon s$, etc). $|n\rangle$ denotes photon states. $\varrho*$ stands for the two complex coordinates of the functions representing the open channels only.

The functions Φ_i and X_j are optimized separately. We call the two spaces spanned by them Q and P, respectively. The convergence of the overall calculation and the accuracy of

the results depend on the quality and on the number of configurations making up Q and P. The configurations in Q or in P space representing bound or quasi-bound N-electron states or bound ionic cores contain orbitals of real coordinates. In general, and especially in open shell systems with low-lying excited states, Q and P should be multidimensional. However, there are also cases where one state or one channel suffices. For example, for a negative ion such as H^-, which does not have bound states, if we neglect the quasibound doubly excited states, Q consists of only the correlated wave function of the ground state, $1s^2$. Similarly, if we compute only the single photoionization cross section, $\sigma^+(E)$, for He-like ground states to the $1s\varepsilon p \ {}^1P^o$ channel (see Sec. III), then the configurations in P would have the same structure, i.e., $1sg_p(\varrho*)$, where the Gamow orbital g_p of p symmetry is expanded in terms of complex basis functions.

The coordinates in the total Hamiltonian operator (atom plus coupling to the external field) are kept real. This fact implies that the difficult electronic structure and electron cor-
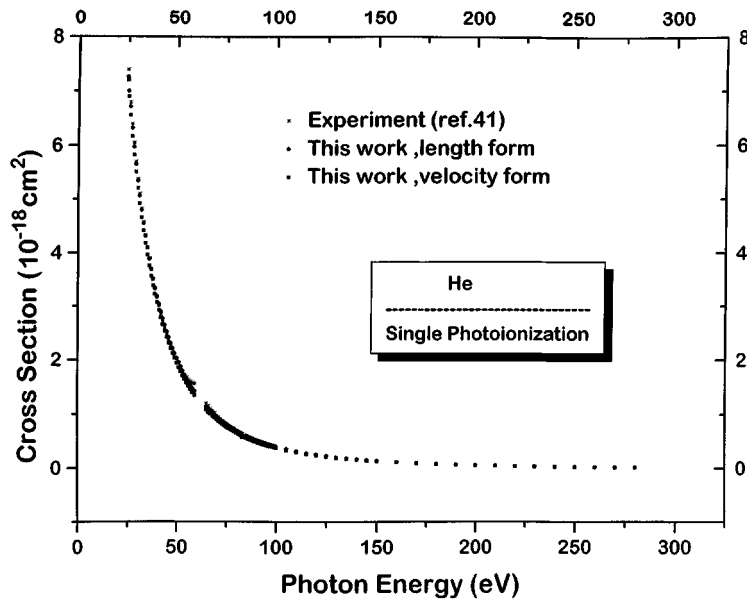
FIG. 1. Single photoionization cross section of He (in 10^{-18} cm^2) as a function of photon energy (in eV). The stars show the experimental values from [41]. The solid circles and squares show our results from the length and velocity forms, respectively. For photon energies between 60 and 65 eV we do not give results since in our calculation the contribution to the single photoionization from the $n=2$ channel and the $2s2p$ state is omitted.

relation calculations for the bound states can be carried out in terms of Hermitian matrices. Furthermore, the open channels can be identified directly.

Once the trial Q and P are chosen, corresponding state-specific non-Hermitian matrices are constructed, containing the free atom interactions in symmetry blocks (S states, P states, D states, etc.) and the corresponding electric-dipole interaction matrices. The explicit form and method of diagonalizing these matrices in the general case (single or multi-photon processes) are given in [28] and hence are not repeated here. The result of diagonalization is a complex eigenvalue for the dressed state of interest, from which either the total width or the partial widths can be deduced. For the present problem, this implies that one can obtain the rates for single ionization, for double ionization, and for double ionization to specific final-state channels ($\varepsilon l \varepsilon' l'$). The corresponding cross sections $\sigma(\omega)$ are given by $\sigma(\omega) = \omega[\Gamma(\omega,F)/\hbar I]$, where $\Gamma(\omega,F)$ is the width for frequency ω and field strength F, and I is the field intensity.

C. Categories of configuration-interaction and computational steps for the calculation of $\sigma^{++}(E)$ for $1s^2 + h\upsilon \rightarrow 2e^-$

Let us define the independent particle approximation to the exact $^1P^o$ two-electron scattering wave function $\Psi(r_1, r_2; E)$, as the symmetrized product of two Coulomb wave functions of s and p symmetry at energies $\varepsilon_1 + \varepsilon_2 = E$. The nuclear charge for each function is the same, since, otherwise, the use of effective charges, i.e., of screening, would imply the application of some model representing electron correlation in the continuum. Let us denote this function by $\Phi_0(sp; E)$. Similar products can be written for (pd), (df), etc. Coulomb orbitals. Since the H$^-$ and He ^1S ground state has, overwhelmingly, $ss + pp$ character, the final-state zeroth-order components that connect via the dipole operator are $\Phi_0(sp; E)$ and $\Phi_0(pd; E)$, each of which defines a Fermi-sea channel.

When electron correlation is considered, the following types of configuration interaction occur: (i) energy-dependent interchannel coupling between the Fermi-sea

channels and between them and additional channels such as the $\Phi_0(df; E)$; (ii) one- and two-electron intrachannel coupling for each Φ_0 and E; (iii) interchannel coupling between the $\Phi_0(\varepsilon_1 l, \varepsilon_2 l'; E)$ and the one-electron channels $\Phi_n(nl, \varepsilon l')$, such as $1s\varepsilon p$, $2s\varepsilon p$, $2p\varepsilon s$, $2p\varepsilon d$, etc.; (iv) interaction between each $\Phi_0(\varepsilon_1 l, \varepsilon_2 l; E)$ and the bound or doubly excited states (DES) below the two-electron ionization threshold I^{++} (when $N>2$, certain DES may in fact occur inside the two-electron continuum of a different threshold).

When the wave function (5) is employed in connection with the overall diagonalization procedure, in principle all of the above mixings are accounted for, to an accuracy determined by the ability of the function space to provide in the complex energy and coordinate planes a good representation of the field-induced resonance wave function and by the power of the numerical techniques.
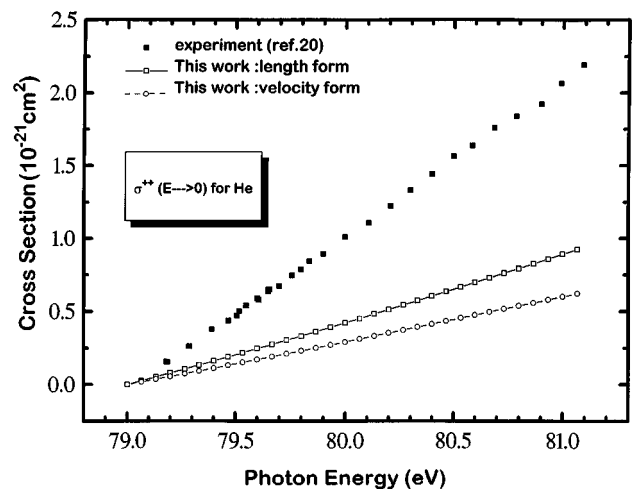

FIG. 2. Double photoionization cross section of He (in 10^{-21} cm^2) as a function of photon energy (in eV) near threshold. The solid squares show the experimental values of Kosmann, Schmidt, and Andersen [20]. The open squares and circles show our results from the length and velocity forms, respectively.
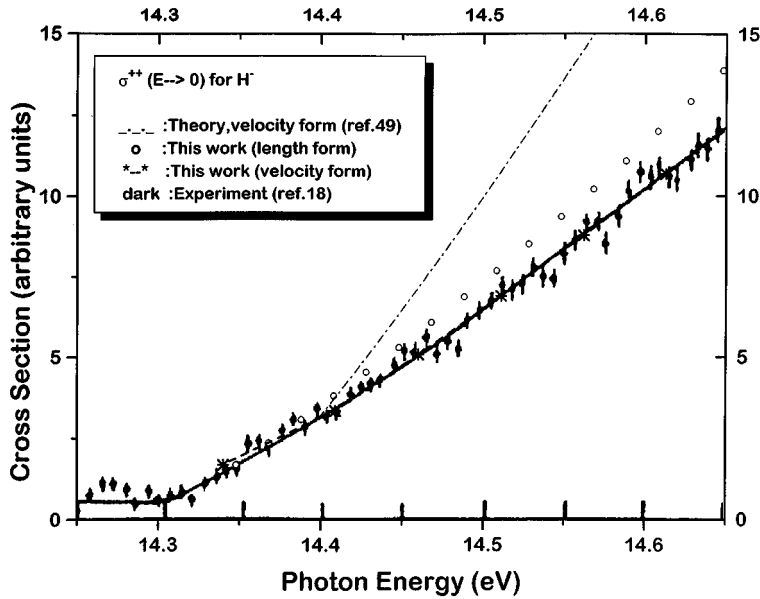
FIG. 3. Double photoionization cross section of H$^-$ (in arbitrary units) as a function of photon energy (in eV) near threshold. The solid line is the fitting through the experimental data (solid circles) of Donahue *et al.* [18]. The dashed-dotted line represents theoretical results by Mc-Cann and Crothers [49] who used the velocity form. The open circles and the stars show our results from the length and velocity forms, respectively. The cross section is equated at photon energy 14.355 eV with that of [18] for reasons of comparison. The same was done for the theoretical results of [49] but for photon energy 14.4 eV.

Of the above four categories, (iii) presents a special conceptual challenge for the following two reasons: (1) When the complex eigenvalue is determined, one must be certain that its imaginary part represents exclusively $\sigma^{++}(E)$ and not a certain sum of $\sigma^{++}(E) + \sigma^+(E)$ (see below). (2) On the other hand, the total wave function at any value of E above I^{++} is a mixture of one- and two-electron scattering channels. This implies that each of the cross sections $\sigma^{++}(E)$ and $\sigma^+(E)$ contains information coming from this mixing.

In order to deal with case (2), we followed our previous proposal of computing partial widths with interchannel coupling to all orders for decay processes such as multichannel autoionization and predissociation via diagonalization of appropriate non-Hermitian matrices with $\mathcal{L}^2$ function spaces [36–38]. This approach requires that first, two independent calculations for the single, $\sigma^+(E)$, and the double, $\sigma^{++}(E)$, cross sections are carried out, and then the corresponding spaces P_1 and P_2 are allowed to mix through the total Hamiltonian in the construction of the full matrix, where the basis sets for P_1 and P_2 are nonorthonormal between them since they are optimized separately. The partial widths are then obtained from the imaginary part of the matrix element $\langle \Psi_0 | \vec{D} | X_i \rangle c_i / c_0$, where Ψ_0 is the initial state, X_i is the wave function for the ith channel, and c_0 and c_i are the coefficients, after diagonalization, of Ψ_0 and of X_i, respectively.

A series of calculations using the $1s\varepsilon p$ channel, which above 80 eV carries more than 90% of the oscillator strength [3,39], exhibited numerical uncertainties coming from the tendency of the continuum functions in P_1 and P_2 to overcomplete the physically significant space. Hence the final results with interchannel coupling were not as stable as desired, especially for small imaginary parts. More work on this problem is needed, with very accurate diagonalizers of large complex matrices and with machines with quadruple precision. Therefore the calculations presented here were done by incorporating the effects of pair correlation of the two free electrons while excluding the contribution of the mixing of P_1 into P_2. They were carried out as follows.

As regards the P space, of the square-integrable X^{++} functions of expression (5), our choice was an expansion over one electron $\mathcal{L}^2$ complex functions, $\widetilde{u}_i$:

$$X^{++}(\rho_1^*, \rho_2^*) = \sum_s \sum_{ij}^M a_{ij}^{(s)}(\theta)[\widetilde{u}_i(\rho_1^*)\widetilde{u}_j(\rho_2^*)]^{(s)}. \quad (6)$$

The index s runs over the different two-electron ionization channels (TEIC's), which, in this application, were chosen as (sp), (pd), and (df). The final calculations were done using Slater orbitals and two nonlinear parameters, α_1 and α_2, one for each electron. Laguerre functions were also tested, but no significant changes were seen.

X^{++} contains terms reflecting the correlation of electronic structure-dependent pairs of electrons, *with a mixture of amplitudes representing equal or unequal sharing of the available total energy*. Its optimization is achieved by repeatedly
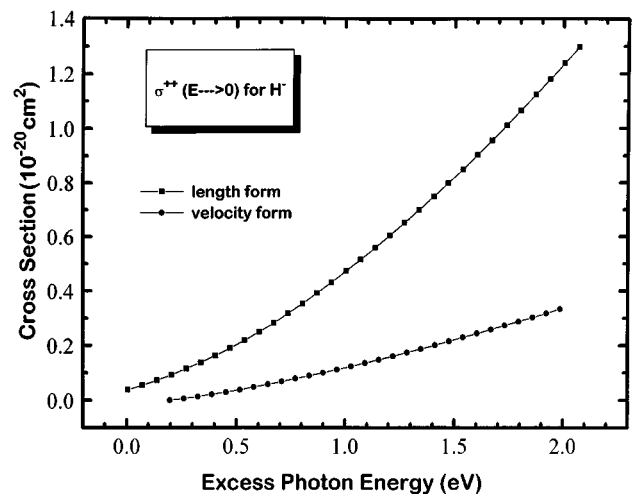

FIG. 4. Double photoionization cross section of H$^-$ (in 10^{-20} cm^2) as a function of excess photon energy (in eV). The solid squares and circles show our results from the length and velocity forms, respectively.
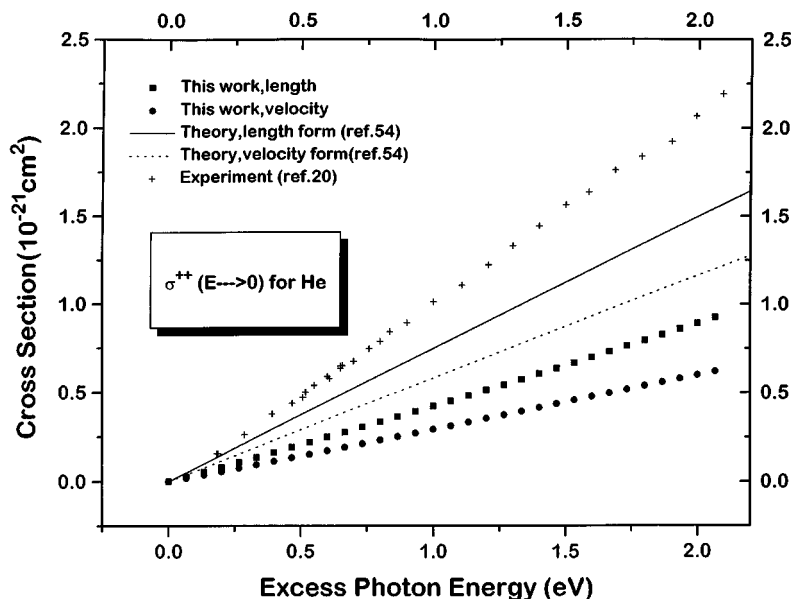
FIG. 5. Double photoionization cross section of He (in 10^{-21} cm^2) as a function of excess photon energy (in eV) near threshold. The stars show the experimental values of Kossmann, Schmidt, and Andersen [20]. The solid and dashed line curves show theoretical results obtained with the golden rule formula and an uncorrelated final-state wave function [54] from the length and velocity forms, respectively. The solid squares and circles show our results from the length and velocity forms, respectively.

diagonalizing the non-Hermitian many-electron, one-photon matrix as a function of the parameters θ, α_1, and α_2, until a stability region is found for the complex eigenvalue z_0 for which the solution Ψ overlaps maximally with Ψ_0.

The quality of the expansion (6) used to express X^{++} in Hilbert space depends on the type of $\widetilde{u}_i$ and on their number M. As with every calculation, the latter is restricted by constraints of numerical accuracy and of computational economy. On the other hand, an additional constraint must be imposed on the $\widetilde{u}_i$, dictated by the requirement that X^{++} should not contain components of the one-electron ionization channels, (OEIC), since, otherwise, the ionization rate determined from the imaginary part of the complex eigenvalue would contain arbitrary contributions from these channels. This exclusion is accomplished by requiring the orthogonality

$$\langle \widetilde{u}_i(\rho^*)/nl \rangle_{r_1 \text{ or } r_2} = 0, \qquad (7)$$

where nl are the hydrogenic orbitals of the most important OEIC's. In the case of polyelectronic atoms, the $|nl\rangle$ represent the appropriate Hartree-Fock orbitals of bound configurations corresponding to one-electron open channels. Similar orthogonality constraints on trial functions have been employed in the theory of autoionizing states [40].

As regards the Q space, two levels [(i) and (ii)] of calculations of $\sigma^{++}(E)$ were carried out. In level (i) the Q space contained only the ground state ^1S, represented by a numerical multiconfiguration Hartree-Fock (MCHF) wave function [30] with configurations $1s^2, 2s^2, 3s^2, 4s^2, 2p^2, 3p^2, 4p^2, 3d^2, 4d^2, 4f^2$. For He this function (such MCHF solutions include the contribution of single excitations) gives an energy of $E_0 = -2.902\,909$ a.u. and for H$^-$ of $E_0 = -0.527\,490$ a.u., sufficiently close to the exact energies $-2.903\,724$ a.u. and $-0.527\,751$ a.u. correspondingly. This choice for Q is equivalent to the use of a ^1S ground-state wave function computed by any method which accounts well for radial and angular electron correlation, in the golden rule approach of Refs. [2, 3, 6, 7, 9–11, 13].
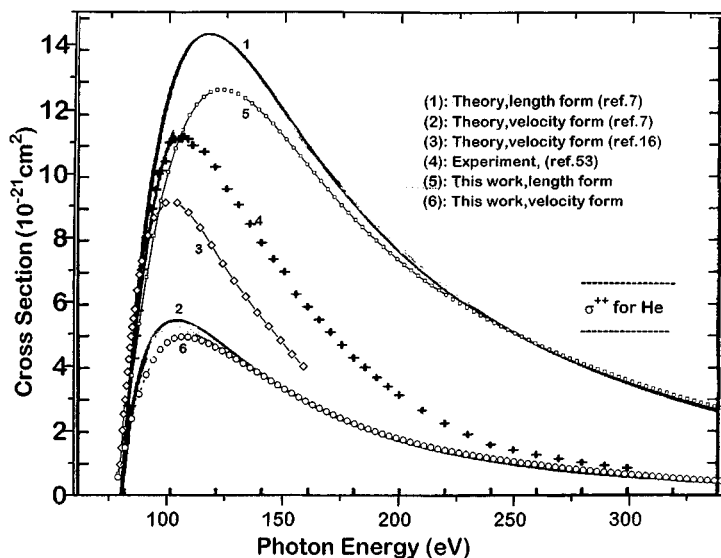

FIG. 6. Double photoionization cross section of He (in 10^{-21} cm^2) as a function of photon energy (in eV). Curves 1 and 2 show theoretical results of LeRouzo and Dal Cappello [7] from the length and velocity forms, respectively. Curve 3 shows theoretical results of Pont and Shakeshaft [16] from the velocity form. Curve 4 shows the experimental values from Bizau and Wuilleumier [53]. Curves 5 and 6 show our results from the length and velocity forms, respectively.
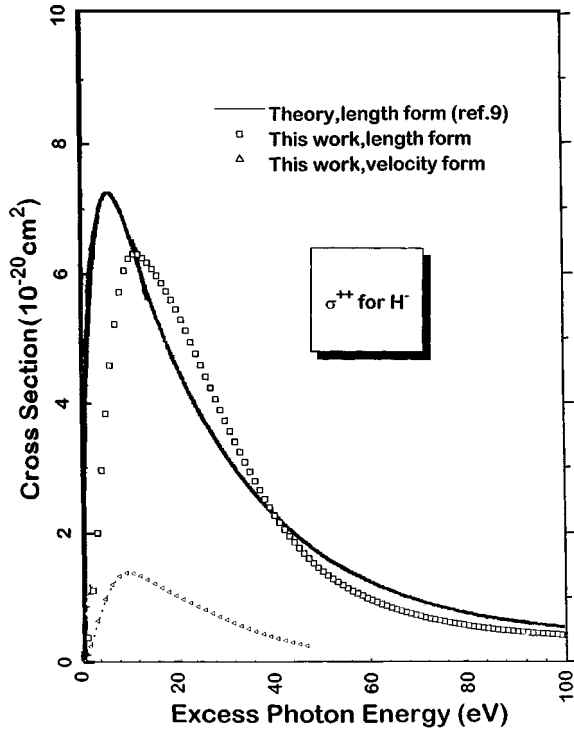
FIG. 7. Double photoionization cross section of H^- (in 10^{-20} cm^2) as a function of excess photon energy. The solid curve shows the theoretical results of Leonardi and Calandra [9] from the length form. The open squares and triangles show our results from the length and velocity forms, respectively.

In level (ii) calculations (done only for He), the Q space was augmented by incorporating low-lying bound excited states and doubly excited autoionizing states. In particular, following the FOTOS analysis of Sec. II, in addition to the Ψ_0 of level (i), the level (ii) Q space contained Hartree-Fock (HF) and MCHF wave functions for the states $1s2s\ ^1S$, $1s2p\ ^1P^o$, $1s3s\ ^1S$, $1s3p\ ^1P^o$, $1s3d\ ^1D$, $(\alpha_1 2s2p + \alpha_2 2p3d)^1P^o$, $(\beta_1 2s^2 + \beta_2 2p^2)\ ^1S$, $(c_1 2p^2 + c_2 2s3d)^1D$, $2s3p\ ^1P^o$, $2p3d\ ^1P^o$, and $2p3s\ ^1P^o$. This function space, covering states of ^1S, $^1P^o$, and ^1D symmetries interacting via the dipole operator, allows the contribution of virtual processes, such as those indicated by expressions (3) and (4).

The results of the calculations that were done according to the above are presented in Secs. IV–VI.

III. SINGLE PHOTOIONIZATION OF He

We already mentioned that, in principle, a complete calculation of the two-electron wave function should include the component of the single-electron channels. In the present case, such channels are the $1s\varepsilon p$, $2s\varepsilon p$, $2p\varepsilon d$, $2p\varepsilon s$, etc., of which the first draws more than 90% of the oscillator strength. We calculated the $\sigma^+(1s^2 \rightarrow 1s\varepsilon p)$ cross section as an independent problem, and compared with the experimental values of Samson *et al.* [41], which were assigned an accuracy of 1–2 % (Ref. [41] cites a large number of previous experimental and theoretical works). The results are presented in Table I and in Fig. 1. The agreement is very good. The Q space consisted of the correlated ^1S ground state and the HF $1s2p\ ^1P^o$ excited state. The P space consisted of ten

configurations $1s\sigma_p$, where σ_p are the Slater-type orbitals of p symmetry and complex coordinate ϱ^*, with optimized exponent 1.10.

IV. APPLICATION TO DOUBLE PHOTOIONIZATION NEAR THRESHOLD. $E = 0.0 - 2.0$ eV

The main motivation for the present work was the long-standing problem of computing quantum mechanically the effects of the pair correlation of two free electrons with total energy E at or just above threshold (say up to $E = 2$ eV).

As regards experiment, it has indeed been possible to measure photoionization cross sections for the emission of two electrons, with E just above threshold [18–21,42–47]. For example, Donahue *et al.* [18] measured this quantity in H^- in arbitrary units. Bae, Coggiola, and Peterson [19] published the first measurements of the absolute cross section close to threshold, $\sigma^{++}(E \rightarrow 0)$, using He^- in the metastable $1s2s2p\ ^4P^o$ state. Finally, Kossmann, Schmidt, and Andersen [20] measured $\sigma^{++}(E \rightarrow 0)$ for He, and fitted it to the Wannier expression for the energy dependence of two-electron ionization at threshold:

$$\sigma^{++}(E \rightarrow 0) = \sigma_0 E^m, \qquad (8)$$

where $\sigma_0 = 1.02 \times 10^{-21}$ cm^2 and $m = 1.05 \pm 0.02$, for E up to 2 eV. They concluded that the experimentally determined range of the validity of Eq. (8) is substantially smaller than previous estimates from the Wannier theory. In addition, they challenged theory toward the first *ab initio* calculation of $\sigma^{++}(E \rightarrow 0)$, given the fact that the related major problem of pair correlation has resisted solution via quantum-mechanical computation for decades.

Ever since the 1950s this problem has been treated by solving approximate equations via classical or semiclassical mechanics (based on truncation of the expansion of the full interaction), following the pioneering work of Wannier [23]. His basic assumptions and mathematical treatment have inspired a number of researchers over the years, whose results, together with the fundamental ones [23], constitute the so-called ''Wannier theory'' [22,24].

As developed and applied, the semiclassical theories cannot address the problem of computing directly $\sigma^{++}(E \rightarrow 0)$. First of all, the calculation of $\sigma^{++}(E)$ requires the calculation of the dipole transition matrix element in the two standard forms (length, velocity) and this implies the systematic incorporation of electron correlation in both final and initial states. Second, the final-state wave function should express the possibility that the total energy above threshold E is allowed to be distributed between the two electrons in the presence of a structured core. [There is no *a priori* reason why the various channels arising from the coupling to a structured core should produce the same energy dependence for $\sigma^{++}(E)$.] Instead, the semiclassical theories have assumed the physically sound Wannier postulate of energy equipartition at $E = 0$ for a structureless core and have produced a general result just for the exponent m of Eq. (8), applicable to double photoionization or electron-impact ionization near threshold, where, apart from the basic approximations, the dependence of the dynamics on the electronic structure of the states involved and on the effect of interchannel coupling to all orders is ignored. For the $^1P^o$ final states of H^- and He,
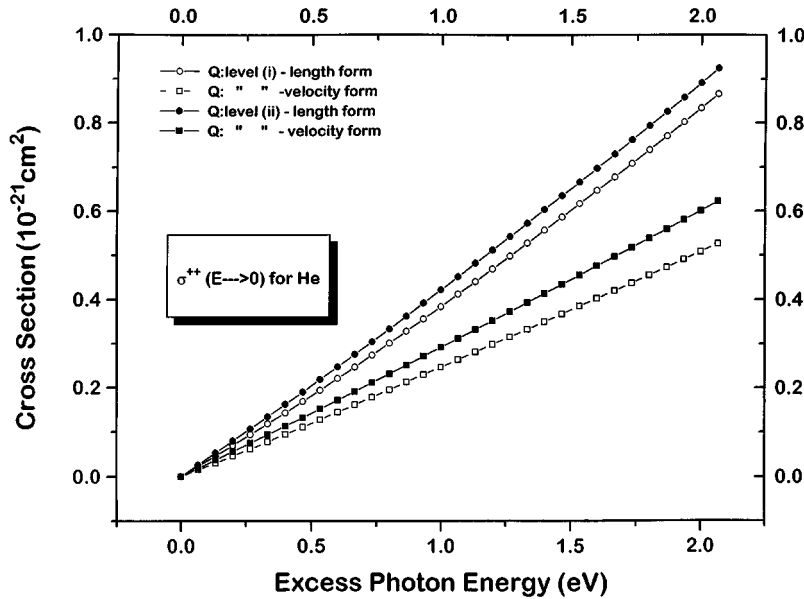
FIG. 8. Double photoionization cross section of He (in 10^{-21} cm^2) as a function of excess photon energy (in eV) near threshold. The open circles and squares show our results from the length and velocity forms where the Q space is at level (i). This means that the Q space contains only the He ground-state correlated wave function (see text). The solid circles and squares show our results from the length and velocity forms where the Q space is at level (ii). The Q space of level (ii) consists of the Q space of level (i) plus a number of singly and doubly excited states (see Sec. II C in text).

the Wannier values for m are [23,48] $m(\text{H})=1.127$ and $m(\text{He})=1.056$, and have become the reference numbers for related work [24,49]. If there is no correlation between the scattered electrons, the energy dependence is linear [50] (see below).

A recent *ab initio* calculation of $\sigma^{++}(E)$ of He by Pont and Shakeshaft [16], where basis sets together with a product of two screened Coulomb functions with effective charges serve as input to a method utilizing a flux formula and information from the asymptotic region, produced results for $E=2$–80 eV. For the low-energy portion, very good agreement with experiment [20] was found. For E below 2 eV, convergence was not achieved. By some kind of extrapolation to the accepted result $\sigma^{++}(0)=0$, they obtained $\sigma_0=0.97\times10^{-21}$ cm^2, in excellent agreement with the experimental value [20]. However, for the high-energy portion, beyond the peak in $\sigma^{++}(E)$ at about 20 eV, the theoretical results deviate from the experimental ones. Note that only the velocity form results were reported.

A. Results

A series of calculations were done, varying the number of M [Eq. (6)] and n [Eq. (7)], and checking for convergence and numerical stability as both increase. Nonorthonormal as well as orthonormal basis functions were employed. Beyond a point, Schmidt orthogonalization introduces numerical inaccuracies, at least for calculations in double precision. The results given here were obtained with $M=6$ and $n=5$, per symmetry, and a common nonlinear parameter α. Close to threshold, for He the (sp) TEIC dominates, with (pd) contributing important corrections. For H$^-$, both sp and pd TEICs are important. The next combination, (df), has a small contribution [51].

We carried out calculations for 50 energy points between 0.02 and 1.0 eV for H$^-$, and for 100 energy points between 0.02 and 2.0 eV for He. The results are plotted in Fig. 2 for He and in Figs. 3 and 4 for H$^-$. The results for He were obtained by subtracting from the calculated cross sections the contribution of the higher single-electron ionization

channels. This contribution is essentially constant for energies between 0 and 2 eV above the two-electron ionization threshold. For both H$^-$ and He, for very small E the imaginary part of the complex eigenvalue contains numerical uncertainties due to the very small values of the rate as it tends to zero. This fact leads to convergence difficulties. For example, in the range (0.0–0.5 eV) the basis set convergence is about 20% whereas for larger energies it is 10% or better. We expect that larger calculations on bigger machines with quadruple precision will reduce this error significantly.

The experimental values of [20] for He refer to absolute cross sections whereas those of [18] for H$^-$ do not. Thus, the comparison on Fig. 3 is constructed by equating our result at 14.355 eV (threshold) with that of [18] and then scaling the rest of our data. The same was done for the formula given in [49] (obtained using the velocity form), $\sigma(E)=3.14\times10^{-20}E^{1.127}$ cm^2, where $m=1.127$ is the classical result of Wannier theory. The reference point was at 14.4 eV. Figure 4 presents the absolute $\sigma^{++}(E)$ for H$^-$. To our knowledge, no other work on *ab initio* theory or experiment exists for this problem.

Finally, given the great interest in the formulation and interpretation of the two-electron threshold ionization process in terms of models and analytic expressions [18–24,49,50,52], we have fitted our results to the Wannier expression [Eq. (8)] as well as to the more flexible one [24,52], cE^m+dE^{m+1}, for the energy ranges (in eV) [0.0, 0.5], [0.0, 1.0], and [0.0, 2.0]. For the larger energy ranges, the second formula produces a better fit. The results of the fitting for m show about a 10% variation, depending on the size of the calculation and on the energy range. For example, in He, for $E=(0.0$–0.5 eV) the present results give $m=1.032$ while for $E=(0.0$–2.0 eV) they give $m=1.060$, in agreement with [20]. Similarly, for H$^-$ in the range 0.0–0.5 eV the fit gives $m=1.20$ and in the range 0.0–1.0 eV it gives $m=1.37$.

B. Comparison with results obtained using an uncorrelated final-state wave function

As already discussed, except for the coupling between the one- and the two-electron channels, the present calculations
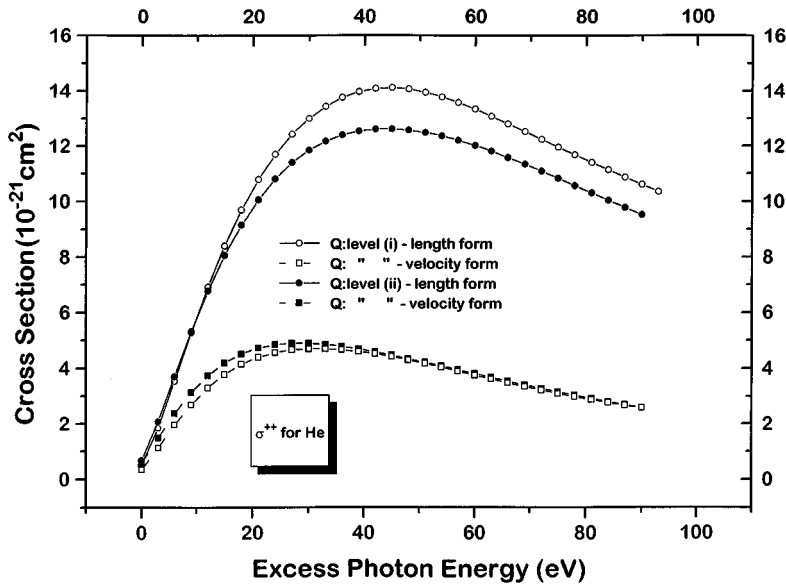
FIG. 9. The same as in Fig. 8 but for excess photon energy far from threshold.

account for pair correlation in the continuous spectrum, to the degree that the function space defined by the Slater complex coordinate orbitals allows.

We considered it useful to compare these results with the ones obtained from a golden rule calculation [54] where the initial-state wave function is the same numerical MCHF function but the final state is uncorrelated, i.e., it is a symmetrized product of Coulomb functions with $Z=2$ (for He).

The results of the two types of calculation for He are compared in Fig. 5, which also contains the experimental values [20]. Of course, the uncorrelated calculation gives the wrong result of a linear dependence on E. On the other hand, it is interesting to observe its proximity to the experimental values. It follows that the bulk of the contribution to $\sigma^{++}(E\to0)$ comes from initial-state Hartree-Fock plus correlation. The contribution of final-state correlation for this system is small as regards the basic features of $\sigma^{++}(E)$ and important only as regards the details (e.g., E dependence close to threshold). Whether this is true for atoms with more complex electronic structures remains to be determined.

V. RESULTS FOR ENERGIES 2–250 eV

The same type of calculations were carried out for He in the range 2–250 eV and for H$^-$ in the range 2–100 eV above threshold. Now, the values of $\sigma^{++}(E)$ are considerably larger and numerical instabilities related to basis set orthogonalities and over-completeness as well as to diagonalization are eliminated. Therefore, these results have converged well, within the function space that is employed.

For He, comparison can be made with the theoretical results of LeRouzo and DalCapello [7] and of Pont and Shakeshaft [16] and with the experimental ones of Bizau and Wuilleumier [53] (Fig. 6). For H$^-$, there are no experimental measurements in this energy range. Figure 7 shows our results together with the theoretical ones of Leonardi and Calandra [9], for which the final state is a product of Coulomb functions.

VI. THE CHOICE OF Q AND THE $\sigma^{++}(E)$ OF He

In Secs. II A and II C we discussed the choice of zero order and correlating configurations for the initial ^1S state as

well as the possible importance of including, through the use of a multidimensional function space Q, higher-order effects. In Figs. 8 and 9 we compare the results for the $\sigma^{++}(E)$ of He from the two choices of Q, level (i) and level (ii), for the energy ranges 0–2 eV and 0–90 eV. There is a small improvement from level (i) to level (ii), which is not sufficient to bring agreement between the results obtained with the length and the velocity forms. The situation may be different in other atoms with low-lying excited states and larger mixing coefficients and oscillator strengths.

VII. CONCLUSION

We have shown how the *ab initio* calculation of the two-electron photoionization cross section, $\sigma^{++}(E)$, near and far from threshold, can account for electronic structure and the various electron correlation effects in initial and final states. The theory is based on the state-specific expansion of the field-induced resonance state given by Eq. (5). Its implementation involves configuration-interaction techniques and this permits the systematic analysis and understanding of the degree of significance of the various interactions due to angular-momentum couplings, to nonorthonormality, to localized correlations, and to intrachannel and interchannel couplings (Secs. II A and II C). The ionization rate is obtained from the imaginary part of the complex eigenvalue of the state-specific non-Hermitian matrix, which is constructed according to the arguments given here and is solved, for single or multiphoton absorption, according to the MEMPT [28]. Using H$^-$ and He as testing grounds, this development allowed the *ab initio* calculation of $\sigma^{++}(E\to0)$ that incorporates electron correlation in both initial and final states. The same method produced $\sigma^{++}(E)$ far from threshold as well as $\sigma^{+}(E)$ to the $1s\varepsilon p$ channel.

The overall performance of the numerical implementation of the theory was quite satisfactory. We expect that larger calculations on better machines will allow experimentation with the $\mathcal{L}^2$ functions of the P space, which account for the contribution of the multichannel outgoing part of the field-

induced resonance state to the generation of the complex eigenvalue of the state-specific non-Hermitian matrix. We also expect that future work will shed further light on questions of numerical accuracy in the calculation of the mixing between one- and two-electron degenerate channels where over-completeness of the basis sets, separately optimized, produced certain instabilities. This mixing was not included in the present calculations, (i.e., the mixing of $\varepsilon_1 l \varepsilon_2 l'$ with $n l \varepsilon_3 l'$), and probably this is the main reason for the discrepancy between the length and the velocity results.

[1] Th. Mercouris and C. A. Nicolaides, Phys. Rev. A **48**, 628 (1993), first applied this approach to the calculation of transition rates of multiphoton, two-electron excitation and ejection, starting from the $2p^2\,^3P$ bound state of H^-.

[2] F. W. Byron and C. J. Joachain, Phys. Rev. **164**, 1 (1967).

[3] R. L. Brown, Phys. Rev. A **1**, 341 (1970); **1**, 586 (1970).

[4] M. S. Yurev, Opt. Spectrosc. **38**, 4 (1975).

[5] S. L. Carter and H. P. Kelly, Phys. Rev. A **24**, 170 (1981); C. Pan and H. P. Kelly, J. Phys. B **28**, 5001 (1995).

[6] S. N. Tiwary, J. Phys. B **15**, L323 (1982); P. L. Altick, Phys. Rev. A **25**, 128 (1982); J. Phys. B **18**, 1841 (1985).

[7] H. LeRouzo and C. Dal Cappello, Phys. Rev. A **43**, 318 (1991).

[8] M. Biagini, Phys. Rev. A **46**, 656 (1992).

[9] S. Leonardi and C. Calandra, J. Phys. B **26**, L153 (1993).

[10] F. Maulbetsch and J. S. Briggs, J. Phys. B **26**, 1679 (1993); M. Brauner, J. S. Briggs, and H. Klar, *ibid.* **22**, 2265 (1989).

[11] K. Hino, Phys. Rev. A **47**, 4845 (1993).

[12] D. Proulx and R. Shakeshaft, Phys. Rev. A **48**, R875 (1993).

[13] M. A. Kornberg and J. E. Miraglia, Phys. Rev. A **48**, 3714 (1993); G. Garibotti and J. E. Miraglia, *ibid.* **21**, 572 (1980).

[14] K. W. Meyer and C. H. Greene, Phys. Rev. A **50**, R3573 (1994).

[15] J.-Z. Tang and I. Shimamura, Phys. Rev. A **52**, R3413 (1995).

[16] M. Pont and R. Shakeshaft, J. Phys. B **28**, L571 (1995).

[17] C. A. Nicolaides, Chem. Phys. Lett. **101**, 435 (1983).

[18] J. B. Donahue, P. A. M. Gram, M. U. Hynes, R. W. Hamm, C. A. Frost, H. C. Bryant, K. B. Butterfield, D. A. Clark, and W. W. Smith, Phys. Rev. Lett. **48**, 1538 (1982).

[19] Y. K. Bae, M. J. Coggiola, and J. R. Peterson, Phys. Rev. A **28**, 3378 (1983).

[20] H. Kossmann, V. Schmidt, and T. Andersen, Phys. Rev. Lett. **60**, 1266 (1988).

[21] B. Möbus, K.-H. Schartner, A. Ehresmann, and H. J. Schmoranzer, Z. Phys. D **30**, 285 (1994).

[22] U. Fano, Rep. Prog. Phys. **46**, 97 (1983).

[23] G. H. Wannier, Phys. Rev. **90**, 817 (1953).

[24] For a review of the predictions of the ''Wannier theory'' and of possible alternative interpretations of the related physics, see M. S. Lubell, Z. Phys. D **30**, 79 (1994).

[25] C. A. Nicolaides and D. R. Beck, Chem. Phys. Lett. **36**, 79 (1975).

[26] *Excited States in Quantum Chemistry*, edited by C. A. Nicolaides and D. R. Beck (Reidel, Dordrecht, 1979), p. 143.

[27] C. A. Nicolaides, J. Phys. B **26**, L291 (1993).

[28] Th. Mercouris and C. A. Nicolaides, J. Phys. B **21**, L285 (1988); **23**, 2037 (1990).

[29] C. A. Nicolaides and S. I. Themelis, Phys. Rev. A **47**, 3122 (1993); **45**, 349 (1992).

[30] C. Froese-Fischer, Comput. Phys. Commun. **14**, 145 (1978).

[31] C. A. Nicolaides, Int. J. Quantum Chem. **60**, 199 (1996).

[32] C. A. Nicolaides, Th. Mercouris, and S. I. Themelis, in *New Methods in Quantum Theory*, edited by C. A. Tsipis, V. S. Popov, D. R. Hershbach, and J. S. Avery (Kluwer, Dordrecht, 1996), p. 135.

[33] M. Bylicki, S. I. Themelis, and C. A. Nicolaides, J. Phys. B **27**, 2741 (1994).

[34] C. A. Nicolaides and D. R. Beck, Phys. Lett. **65A**, 11 (1978); C. A. Nicolaides, H. J. Gotsis, M. Chrysos, and Y. Komninos, Chem. Phys. Lett. **168**, 570 (1990).

[35] M. Dörr, J. Purvis, M. Terao-Dunseath, P. G. Burke, C. J. Joachain, and C. J. Noble, J. Phys. B **28**, 4481 (1995).

[36] C. A. Nicolaides and Th. Mercouris, Phys. Rev. A **32**, 3247 (1985); **36**, 390 (1987).

[37] M. Chrysos, Y. Komninos, Th. Mercouris, and C. A. Nicolaides, Phys. Rev. A **42**, 2334 (1990).

[38] I. D. Petsalakis, Th. Mercouris, G. Theodorakopoulos, and C. A. Nicolaides, Chem. Phys. Lett. **182**, 561 (1991).

[39] J. A. R. Samson, quoted in [3].

[40] C. A. Nicolaides, Phys. Rev. A **6**, 2078 (1972).

[41] J. A. R. Samson, Z. X. He, L. Yin, and G. N. Haddad, J. Phys. B **27**, 887 (1994).

[42] G. C. King, M. Zubek, P. M. Putter, F. H. Read, A. A. MacDowell, J. B. West, and D. M. P. Holland, J. Phys. B **21**, L403 (1988).

[43] P. Lablanquie, K. Ito, P. Morin, I. Nenner, and J. H. D. Eland, Z. Phys. D **16**, 77 (1990).

[44] R. I. Hall, L. Avaldi, G. Dawber, M. Zubek, K. Ellis, and G. C. King, J. Phys. B **24**, 115 (1991).

[45] O. Schwarzkopf, B. Krässig, J. Elmiger, and V. Schmidt, Phys. Rev. Lett. **70**, 3008 (1993).

[46] J. C. Levin, G. B. Armen, and I. A. Sellin, Phys. Rev. Lett. **76**, 1220 (1996).

[47] S. J. Schaphorst, A. Jeau, O. Schwarzkopf, P. Lablanquie, L. Andric, A. Huetz, J. Mazeau, and V. Schmidt, J. Phys. B **29**, 1901 (1996).

[48] T. A. Roth, Phys. Rev. A **5**, 476 (1972).

[49] J. F. McCann and D. S. F. Crothers [J. Phys. B **19**, L399 (1986)], using a semiclassically derived wave function together with a previously published well-correlated wave function for the ground state of H^- [M. Rotenberg and J. Stein, Phys. Rev. **182**, 1 (1969)], obtained (in the velocity form) $\sigma_0(H^-) = 3.14 \times 10^{-20}$ cm^2, with m being the Wannier exponent, 1.127, and E given in eV.

[50] Using the alternative assumption of unequal energy sharing

and a Coulomb dipole ansatz, A. Temkin [Phys. Rev. Lett. **49**, 365 (1982); M. K. Srivastava and A. Temkin, Phys. Rev. A **43**, 3570 (1991)] have argued for a different threshold expression, involving logarithmic and modulation factors.

[51] If we were to deal with an $N > 2$ electron system where the final state has a term-dependent electronic structure, X^{++} of Eq. (6) would represent a symmetry adapted product of the complex functions $u_i(\varrho^*)$ with correlated $(N-2)$ core functions of real coordinates.

[52] M. S. Lubell, Phys. Rev. A **47**, R2450 (1993).

[53] J. M. Bizau and F. J. Wuilleumier, J. Electron Spectrosc. Relat. Phenom. **71**, 205 (1995).

[54] C. Sinanis and C. A. Nicolaides (unpublished).